Hindawi
Geofluids
Volume 2022, Article ID 6856298, 11 pages
https://doi.org/10.1155/2022/6856298

Research Article

Remaining Oil Distribution and Development Strategy for Offshore Unconsolidated Sandstone Reservoir at Ultrahigh Water-Cut Stage

Chen Liu,[1,2] **Wensheng Zhou**,[1,2] **Junzhe Jiang**,[1,2] **Fanjie Shang**,[3] **Hong He**,[4] **and Sen Wang**[5]

[1]*State Key Laboratory of Offshore Oil Exploitation, Beijing 100028, China*
[2]*CNOOC Research Institute Ltd., Beijing 100028, China*
[3]*CNOOC International Limited, Beijing 100028, China*
[4]*College of Petroleum Engineering, Yangtze University, Wuhan 430100, China*
[5]*China University of Petroleum (East China), Qingdao, Shandong 266580, China*

Correspondence should be addressed to Chen Liu; liu099339@163.com and Hong He; hehong1103@163.com

Received 8 March 2022; Revised 17 July 2022; Accepted 23 July 2022; Published 6 September 2022

Academic Editor: Jinjie Wang

Due to the influence of long-term waterflooding, the reservoir physical properties and percolation characteristics tend to change greatly in offshore unconsolidated sandstone reservoirs at ultrahigh water-cut stage, which can affect the remaining oil distribution. Remaining oil characterization and proper development strategy-making are of vital importance to achieve high-efficiency development of mature reservoirs. The present numerical simulation method is difficult to apply in reservoir development due to the problems of noncontinuous characterization and low computational efficiency. Based on the extended function of commercial numerical simulator, the time-varying equivalent numerical simulation method of reservoir physical properties was established, and the research of numerical simulation of X offshore oilfield with 350,000 effective grids was completed. The results show that the time-varying reservoir properties have a significant impact on the distribution of remaining oil in ultrahigh water-cut reservoir. Compared with the conventional numerical simulation, the remaining oil at the top of main thick reservoir in X oilfield has increased by 18.5% and the remaining oil in the low-permeability zone at the edge of the nonmain reservoir has increased by 27.3%. The data of coring well and the implementation effect of measures in the X oilfield are consistent with the recognition of numerical simulation, which proves the rationality of numerical simulation results. The new method is based on a mature commercial numerical simulator, which is easy to operate and has reliable results.

1. Introduction

Remaining oil recognition is of vital importance to achieve high-efficiency development for mature waterflooding reservoirs with high water cut. Different analysis methods such as reservoir simulation, dynamic analysis, well logging analysis, and core analysis have been applied to recognize the remaining oil [1]. Among them, reservoir simulation has become a widely used method because it is quantifiable, visualizable, and low cost. Normally, the reservoir simulation is based on a geological model with determined physical parameters such as permeability and porosity. Parameters such as the relative permeability are calculated from the input curves. It is assumed that the determined parameters and input curves do not change during the simulation process [2]. However, during the ultrahigh water-cut development stage for unconsolidated sandstone reservoir in offshore oilfields, after long-term waterflooding, the microscopic pore-throat structure and clay content of the

reservoir will change and affect the flow of water and oil in porous media, which can have an impact on the distribution of remaining oil [3–6].

The existence of the phenomenon has been confirmed by laboratory experiments. Laboratory microscopic tests have confirmed that with the increase of water injection, the clay minerals in pores are continuously washed away by the injected water so that the shale content in the formation decreases. The secondary intergranular voids are more developed and the extralarge intergranular voids also increase [7–9]. Larger pores and throats are constructed in the medium-coarse sandstone, while pore size and throat size decrease in the silty sandstone. After long-term waterflooding, core flooding experiments show that the permeability of high-permeability cores increases and the relative permeability curve moves to the right. The residual oil saturation decreases while the irreducible water saturation increases. The oil saturation range with a two-phase flow increases. The water-phase permeability at residual oil saturation decreases. However, the permeability of the medium and low permeability cores decreases after long-term waterflooding.

The water-phase relative permeability curve shifts to the right, and also, the irreducible water saturation increases. The two-phase flow saturation range shrinks [10–12]. Besides, the well logging data from Daqing, Shengli, and other oilfields at different development stages confirm that the permeability in the medium- and high-permeability sandstone reservoirs gradually increases during waterflooding process [13, 14]. The migration simulation results of reservoir particles [15–17] based on the network modeling show that the changes of reservoir physical properties are mainly affected by factors such as injection pore volume, injection rate, fluid viscosity, degree of reservoir cementation, and clay content.

The change of the reservoir's microscopic pore-throat structure is represented by the change of parameters such as reservoir permeability, porosity, and relative permeability curve in the reservoir simulation. Previous studies indicate that reservoir porosity changes slightly during long-term waterflooding, and its impact on reservoir production can be ignored. Reservoir permeability and relative permeability curves change significantly during waterflooding and have significant impact on production. They are the two main parameters to be considered as the time-varying properties in reservoir simulation [18, 19].

The construction of time-varying reservoir simulation parameters is mainly to determine the variation law of reservoir parameters during the development process. Therefore, the proper characterization parameters of the reservoir development process are particularly important. The water cut of the reservoir has been used as time-varying reservoir simulation parameter [18]. However, the characterization method based on water-cut changes has the following problems: when the reservoir enters into high water-cut development period, although the water cut of reservoir changes slightly, the injection water can have a strong wash effect on the reservoir and the time-varying reservoir simulation parameters change dramatically, which leads to a larger simulation error.

In order to properly characterize the change of reservoir physical properties, the water-pass multiple was proposed [20, 21]. However, the time-varying characterization method based on the water-pass volume multiple cannot eliminate the influence of grid size. For grids of different sizes, the amount of water flowing through the cross-section can be obviously different under the same water-pass volume multiple. To solve this problem, the concept of surface flux (PV/S) [22, 23] is proposed in this paper, which is the flow through a unit flow cross-sectional area. The calculation of the time-varying reservoir simulation properties can be realized by characterizing the quantitative relationship between reservoir parameters and surface flux.

Traditional commercial reservoir simulators do not consider the time-varying reservoir properties. In order to characterize the time-varying phenomenon, some approximate methods are proposed. The segmental simulation method has been proposed [24–29], which divides the simulation process into several time intervals and approximates time varying by setting different property values in each time interval. This method has a discontinuous calculation process and convergence problem. A numerical simulator that considers the time-varying phenomenon has been developed in the literature [30–37]. However, it is difficult to apply to the field case due to low computational efficiency and incomplete description of the physical model.

The time-varying phenomenon by using water-sensitive functions in the commercial numerical simulators was approximately characterized [37–44]. However, the conversion process is complex and the reliability is poor, which is difficult to accurately reflect the time-varying law of reservoir parameters. Due to the limitation of previous methods, the time-varying phenomenon has not been fully considered in reservoir simulation, which resulted in the low accuracy of remaining oil identification in the ultrahigh water-cut reservoirs. It is difficult to further improve the oil recovery without a high-quality simulation result.

Therefore, in this study, taking the example of X offshore oilfield, the X oilfield's geological properties and the time-varying reservoir properties were firstly introduced. Then, a simulation method with time-varying reservoir properties was established, and the distribution of the remaining oil in this oilfield was given. Finally, the development strategies were proposed and the field implementation was tracked.

The numerical simulation of the X oilfield with the time-varying reservoir properties has been achieved based on a commercial numerical simulator, which reveals the remaining oil distribution in the X oilfield. Compared with the results of remaining oil distribution given by conventional numerical simulation, the time-varying simulation results have been confirmed to be more consistent with the real situation of the reservoir. It also has higher accuracy and reliability. The field practice of the X oilfield provides a useful guidance for the EOR strategy-making workflow in the ultrahigh water-cut offshore unconsolidated sandstone reservoirs. Based on the development example of X oilfield, it

is suggested that sufficient attention should be paid to the time-varying reservoir properties to investigate the remaining oil distribution in mature oilfields at ultrahigh water-cut development stage. Moreover, the time-varying simulation method with higher accuracy and reliability should be paid special attention.

2. Characterization of Time-Varying Reservoir Property

The reservoir lithology of the X oilfield is relatively simple, dominated by fine-medium-grained feldspar quartz sandstone, followed by coarse-medium-grained feldspar lithic quartz sandstone and fine-medium-grained quartz sandstone, with the porosity of 18%-25%; the permeability is between 200~1000 ($\times 10^{-3}\ \mu m^2$); it belongs to medium-high porosity and medium-high permeability reservoir. The oil-water distribution in the oilfield is mainly controlled by the structure, and it belongs to the anticline structural reservoir. There are 23 oil reservoirs in the vertical direction, mainly layered edge-water reservoirs. The oilfield has been exploited for nearly 20 years, the oil recovery has reached 55%, and the water cut has reached 95%. It has entered the middle and late stages of development with high water-cut and high recovery ratio. The remaining oil is highly dispersed, and it is difficult for further development.

2.1. Characterization of Time-Varying Permeability. Based on the core flooding experiment, the quantitative relationship between the varying factor of reservoir permeability (the ratio of actual permeability to initial permeability) and surface flux is obtained through statistical regression (Figure 1). Combined with the analysis of well logging interpretation in different development periods, it is believed that the quantitative relationship accurately and objectively reflects the long-term waterflooding variation of reservoir permeability. The logging interpretation results of different periods are basically distributed on the relationship curve, which shows a good agreement with this quantitative relationship. The X oilfield has a complete geological structure, in which there are no faults. Reservoirs distribute stably laterally with good continuity and weak heterogeneity. The interlayer differences are also small, so this time-varying pattern is universal in the X oilfield. Moreover, core flooding experimental results show that the porosity of the core is 23.0% when the surface flux is 150, which is only 2.0% higher than the initial porosity. The result is consistent with the conclusions from Song et al. [6], Chen et al. [7], and others. This change has no significant impact on reservoir development.

However, it can be seen from Figure 1 that the reservoir permeability of the X oilfield increases gradually with the increase of the surface flux. The reservoir permeability in the strong displacement zone is more than 4 times higher than the initial permeability, which is consistent with the understanding from Shengli, Daqing, and other oilfields [13, 14, 28]. It indicates that reservoir heterogeneity becomes more serious during the process of oilfield development.

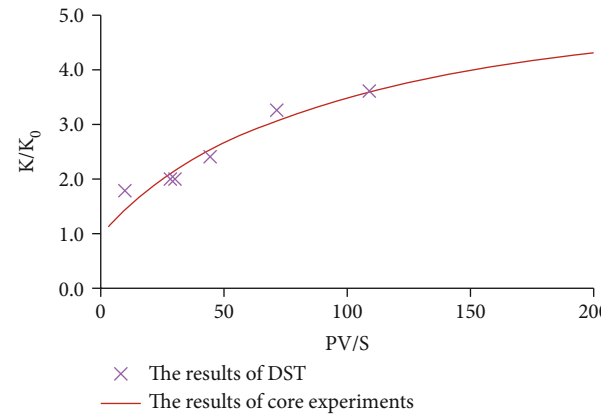

Figure 1: Time varying of reservoir permeability in the X oilfield.

2.2. Characterization of Time-Varying Relative Permeability. The time-varying characterization of relative permeability curve can be achieved by comparing the four endpoint values (initial water saturation S_{wi}, oil phase relative permeability $K_{ro}(S_{wi})$ at initial water saturation, residual oil saturation SOWCR, and the relative permeability $K_{rw}(S_{or})$ at residual oil saturation). Considering the degree of influence on the law of the oil-water percolation, to simplify the problem, the residual oil saturation and the endpoints of the water relative permeability at residual oil saturation are characterized [29, 30]. It can be achieved by constructing the residual oil saturation and the quantitative relationship between the relative permeability of the water phase and the areal flux at the residual oil saturation.

The core flooding experiments of the X oilfield show that long-term waterflooding will lead to a decrease in residual oil saturation, and the relative permeability of the water phase increases at residual oil saturation. However, due to the limited number of data points, it is difficult to conclude to a quantitative formula. In this paper, the reservoir engineering method is used to calculate the changing trend of relative permeability curves [30, 31]. This method firstly obtains the relationship between oil-water two-phase relative permeability ratio and water saturation through waterflooding curve and production data. Then, the exponential expression of the oil-water relative permeability is converted to a binary linear equation by applying the logarithm on both sides. In the next step, the established relationship between oil-water two-phase relative permeability ratio and water saturation is used to obtain the oil-phase index, water-phase index, and water-phase relative permeability under residual oil saturation with binary linear regression. Therefore, the exponential expression of the oil-water relative permeability can be obtained. According to field production data, the relative permeability curves of oil and water at different development stages are calculated by subsections, the relative permeability curve clusters are obtained, and then, the residual oil saturation and the water-phase relative permeability at the residual oil saturation are calculated by the regression (Figure 2).

With the increase of surface flux, the residual oil saturation of the X oilfield shows a gradual downward trend, and

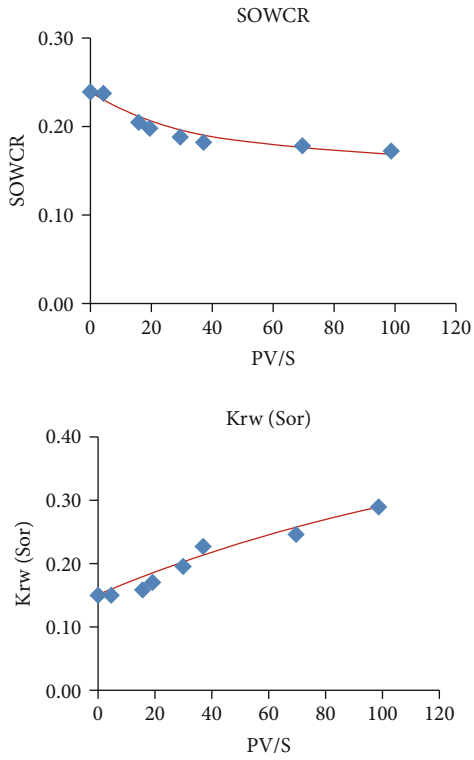

Figure 2: Time varying of relative permeability curve in the X Oilfield.

the residual oil saturation of the strong displacement zone can decrease from initial 0.24 to 0.18, a decrease of 25%. The relative permeability of the water phase at residual oil saturation increases with the increase of surface flux, showing a gradually increasing trend. The relative permeability of the water phase at residual oil saturation in the intensive flooding zone can increase by 93%, from initial 0.15 to 0.29. It indicates that with the deepening of oilfield development, the internal flow pattern of reservoir has changed significantly in comparison with the initial period of development. Compared with the previous research results from Shengli, Daqing, and other oilfields ([28], [14], etc.), the variation range of two endpoints (residual oil saturation and water-phase relative permeability at residual oil saturation) is more obvious under high-intensity waterflooding.

3. Remaining Oil Distribution considering the Time-Varying Properties

3.1. Realization of Reservoir Simulation with Time-Varying Properties. Based on INTERSECT, a widely used commercial numerical simulator, the study of the remaining oil distribution in the X oilfield is completed. The time-varying characterization of permeability can be achieved by adjusting the multiplication factor (MULTX, MULTY). Based on the quantitative relationship between permeability varying factor and surface flux, the characterization formula for quantitative relationship between the multiplication factors with surface flux is obtained. INTERSECT software provides a software script expansion window. PV/S is first calculated based on the default parameters of the software. Then, input the time-varying value of the reservoir's physical properties by script, and specify the value for each step calculation, so that time-varying intergrid conductivity can be realized, and the dynamic real-time calculation of permeability is achieved. The conductivity calculation in the software is based on equation (1). In the above-mentioned time-varying method of reservoir physical properties, the multiplication factor has a cumulative effect. Thus, the multiplication factor needs to be restored to the initial value before calculating the conductivity at each time step. Table 1 is a comparison table of differences in conductivity calculation. It can be seen from Table 1 that if the cumulative effect is not eliminated, the result will obviously deviate from the accurate value.

$$\mathrm{TRANX}_i = \frac{\mathrm{CDARCY} \cdot \mathrm{MLTX}_i \cdot A \cdot \mathrm{DIPC}}{B}, \quad (1)$$

where TRANX_i is transmissibility between cell i and cell j, its neighbor in the positive X-direction; CDARCY, Darcy's constant; MLTX_i, transmissibility multiplier for cell I; A, interface area between cell i and j; DIPC, Dip correction; and B, planar permeability mean of cell i.

At the same time, the quantitative characterization formulas of residual oil saturation, water-phase relative permeability at residual oil saturation, and surface flux are written into the software's script editor with Python to achieve the dynamic calculation of oil-water relative permeability curve for each grid, so as to realize the time-varying characterization of oil-water relative permeability for all grids.

The production of the X oilfield has lasted for nearly 20 years, and the number of effective grids of the model was 350,000. Using the method proposed in this paper and based on INTERSECT simulator, the time-varying numerical simulation of the X oilfield has been completed in the order of whole area history matching-main production well history matching-nonmajor production well history matching. After considering the time-varying reservoir parameters, the efficiency of history matching has been significantly improved. The field production results of the simulation model in the early time steps are basically consistent with the actual production data. And only a few wells need to be properly adjusted to complete the history matching work in the later time step. At the same time, the accuracy of time-varying simulation's history matching has been significantly improved, especially in the production fluctuation period and the later period of development (Figure 3). It has achieved precise characterization of some small areas and solved the problem of water cut rising too fast, in which the original conventional simulation has always existed.

In the conventional reservoir numerical simulation, parameters such as conductivity, residual oil saturation, and water relative permeability at residual oil saturation are usually unchanged during the whole simulation process and are always the initiated values. In the numerical simulation considering time-varying reservoir physical properties, the above values will show dynamic changes with the process of reservoir development. Figure 4 shows the

Table 1: The differences of transmissibility with two methods.

Calculation step	PV/S	Transmissibility (actual)	Cumulative effect		Eliminate cumulative effects	
			MULTX	Transmissibility by the model	MULTX	Transmissibility by the model
Initial value	0	1	1	1	1	1
Step 1	10	1.1	1.1	1×1.1	1.1	$1 \times 1.1/1$
Step 2	20	1.2	1.2	$1 \times 1.1 \times 1.2$	1.2	$1.1 \times 1.2/1.1$
Step 3	30	1.3	1.3	$1 \times 1.1 \times 1.2 \times 1.3$	1.3	$1.2 \times 1.3/1.2$
Step 4	40	1.4	1.4	$1 \times 1.1 \times 1.2 \times 1.3 \times 1.4$	1.4	$1.3 \times 1.4/1.3$
Step 5	50	1.5	1.5	$1 \times 1.1 \times 1.2 \times 1.3 \times 1.4 \times 1.5$	1.5	$1.4 \times 1.5/1.4$

Note: take the formula transmissibility = 1 + (PV/S)/100 as an example.

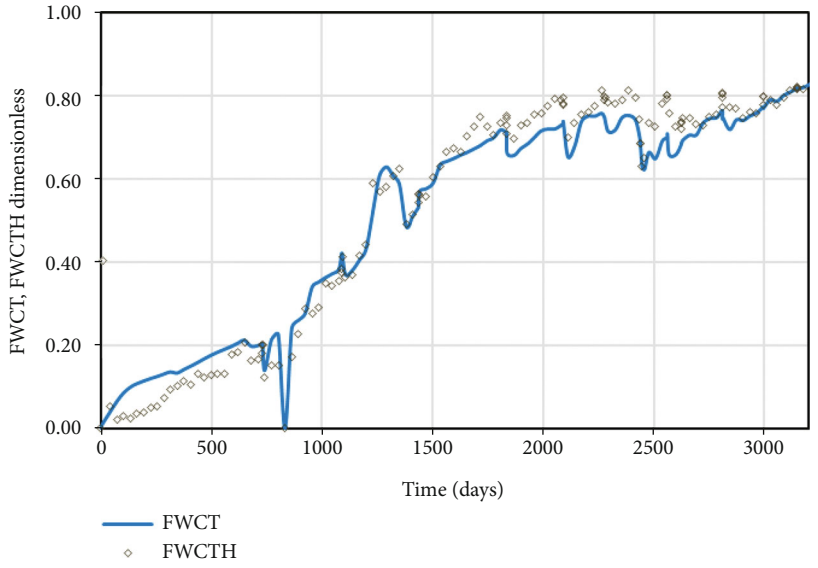

Figure 3: The historical matching results of the X oilfield.

comparison of parameter differences at the beginning and the end of time-varying simulation. It can be seen from Figure 4 that the proportion of grids with a conductivity value greater than 50 in the whole area increases from 3.8% at the beginning to 13.1% at the end, which indicates that the grid conductivity increases during the model operation. The residual oil saturation and the relative permeability of the water phase at residual oil saturation are the same constant value in all grids at the beginning of the model and show obvious heterogeneity at the end of the simulation, which also indicates that these two parameters show time-varying in the process of model running.

3.2. Remaining Oil Distribution Recognition

3.2.1. The Main Oil Group. ZJ-1 oil group is the main oil group in the X oilfield with sufficient edge water energy. Permeability in this group is between 500 and 1000 ($\times 10^{-3}$ μm^2). The geological reserves of this oil group are 1132×10^4 m^3. The current oil recovery is 61%. The comprehensive water cut is 96%. And 15 wells are in production.

Based on the time-varying reservoir simulation results, the remaining oil in the ZJ-1 oil group is mainly enriched in the structural high area, which is basically consistent with the conventional simulation results. However, there are differences in the enrichment degree in the structural high area. According to simulation results (Figure 5), the remaining geological reserves in the structural high area calculated by the conventional simulator are 200×10^4 m^3, of which the movable oil reserves are 132×10^4 m^3, while the remaining geological reserves in the structural high area of the reservoir obtained by the time-varying simulator technology are 237×10^4 m^3, of which the movable oil reserves were 186×10^4 m^3, an increase of 18.5% and 40.9%, respectively.

From the time varying of reservoir parameters during numerical simulation calculation (Figure 6), it can be seen that the middle and lower part of the ZJ-1 oil group is a strong displacement zone with a large surface flux. During the conventional numerical simulation calculation process, the reservoir conductivity and residual oil saturation are constant. In the process of time-varying simulation, the conductivity in the middle and lower part of the reservoir will

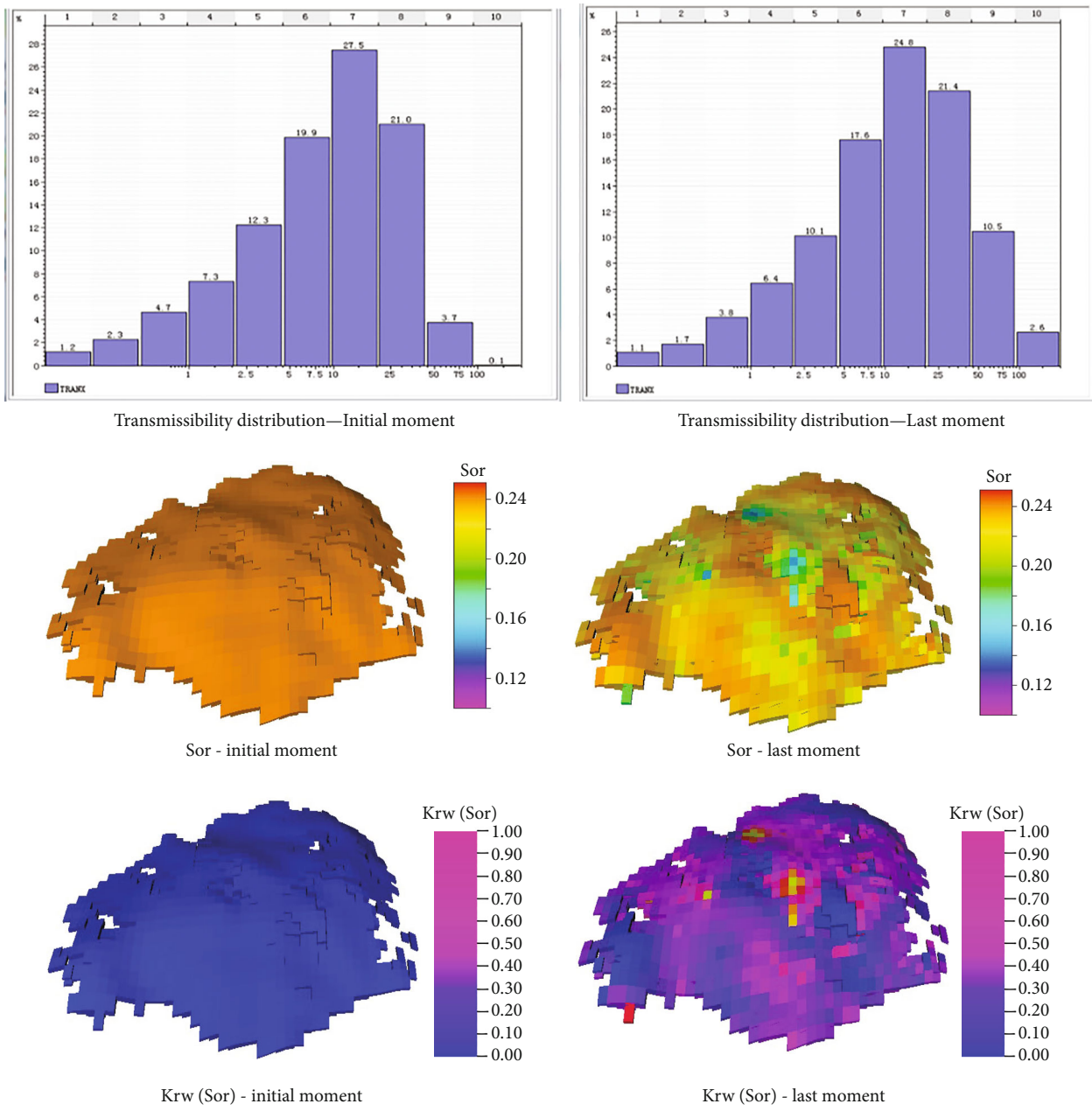

Figure 4: Comparison of parameters at the beginning and the end of time-varying numerical simulation.

gradually increase, and the residual oil saturation will gradually decrease, resulting in a higher recovery ratio in the middle and lower part of the reservoir than conventional numerical simulation. Therefore, the remaining oil is more enriched in the structural high area with a relatively low displacement degree.

3.2.2. Nonmain Oil Groups. Among the 23 oil groups in the X oilfield, except for the ZJ-1 oil group, the rest are all nonmain oil groups. The geological reserves of these oil groups are small, and there are certain differences in the physical properties between these oil groups. Taking the ZJ-2 oil group as an example, the edge water energy of this oil group is sufficient, the permeability is between 200 and 1000 ($\times 10^{-3}$ μm^2), and the physical properties of the eastern part of the reservoir are relatively poor. The geological reserves of this oil group are 110×10^4 m^3, the current recovery ratio is 43%, the comprehensive water cut is 92%, and the production has been stopped.

It can be seen from Figure 7 that the distributions of remaining oil obtained from the traditional and time-varying simulators are basically the same and both show that there is still a certain number of recoverable reserves in the area with relatively poor physical properties in the eastern part of the reservoir. According to simulation results, the remaining geological reserves in this area calculated by conventional simulation are 24×10^4 m^3, of which the movable oil reserves are 16×10^4 m^3, while the remaining geological

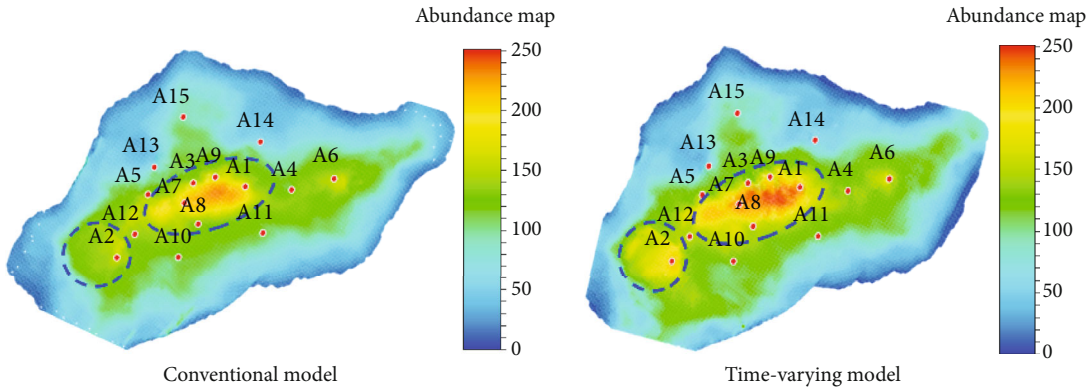

Figure 5: Abundance map of remaining geological reserves of ZJ-1 oil formation.

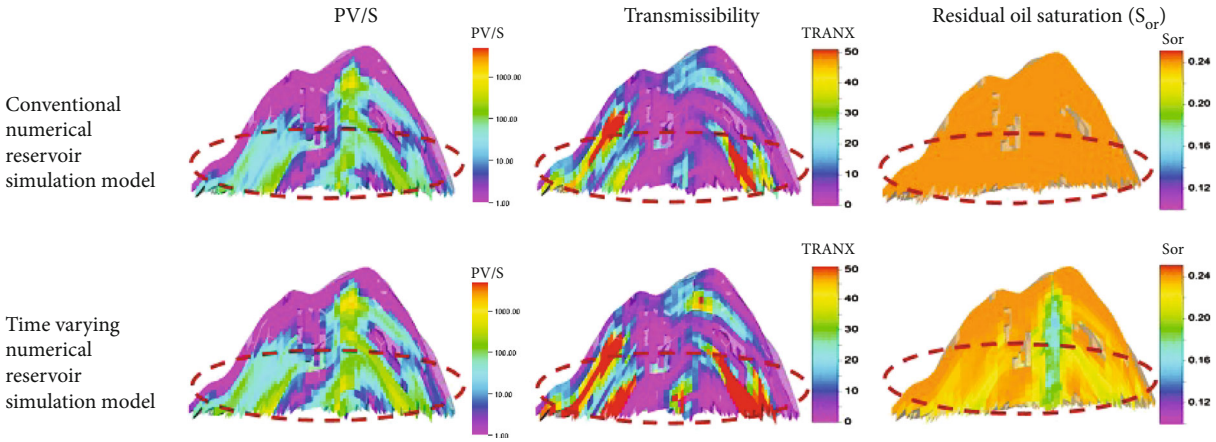

Figure 6: Comparison of reservoir parameters of ZJ-1 oil formation (at the end of model operation).

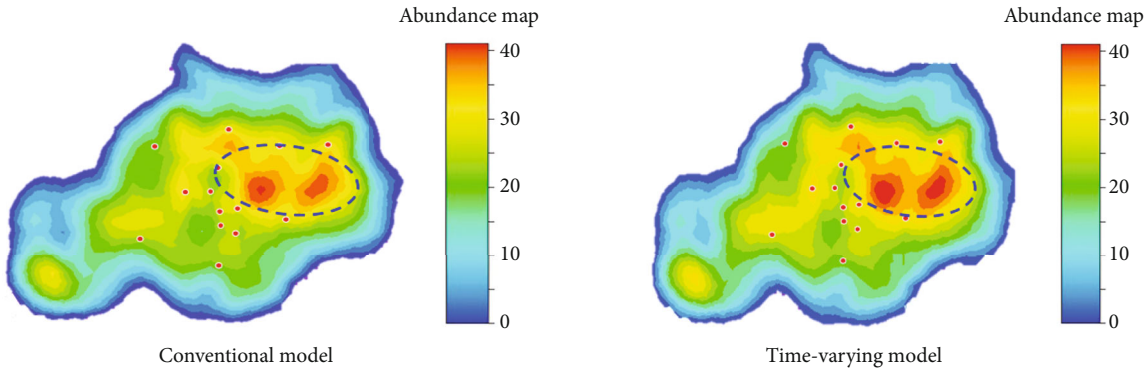

Figure 7: Abundance map of remaining geological reserves of ZJ-2 oil formation.

reserves in this area obtained by the time-varying simulation are 31×10^4 m^3, of which the movable oil reserves are 31×10^4 m^3. Oil reserves are 25×10^4 m^3, an increase of 27.3% and 52.8%, respectively. Based on the remaining oil from the time-varying numerical simulation results, this area still has the potential for adjusting wells.

From the time-varying of reservoir parameters during the simulation (Figure 8), it can be seen that the high permeability zone of the ZJ-2 oil group is a strong displacement zone, and the surface flux is relatively large, so the conductivity of the high permeability zone during the time-varying simulation process will be gradually increased, while the residual oil saturation gradually decreases. So, the recovery ratio of the high permeability zone is higher than that in the conventional simulation results, and the remaining oil is more enriched in the low permeability area with a relatively low displacement degree.

3.3. Development Strategies and Field Implementation Tracking. According to the distribution of remaining oil,

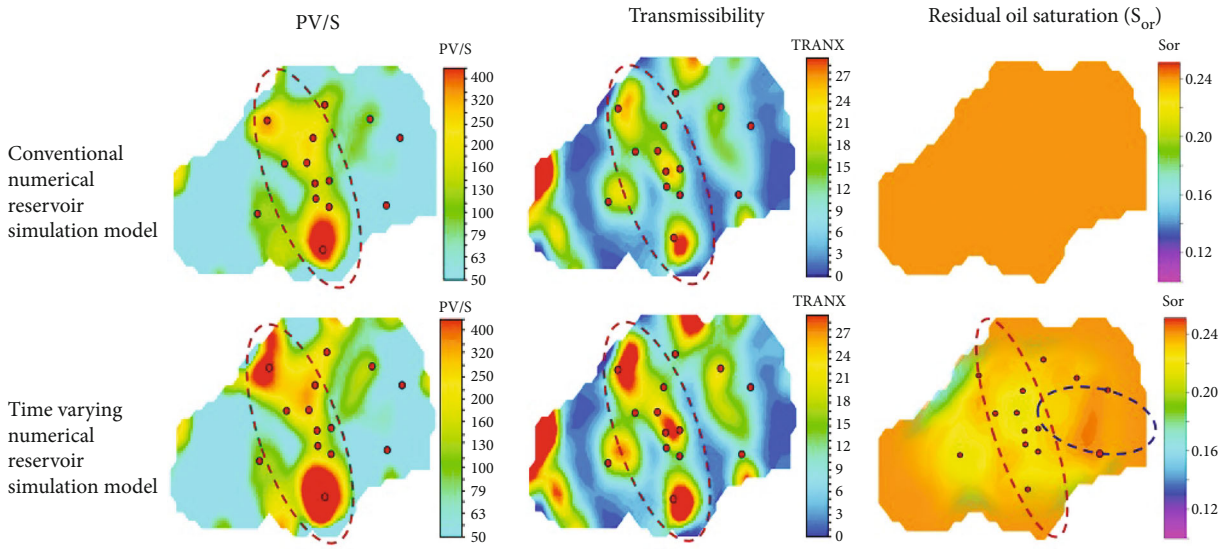

Figure 8: Comparison of reservoir parameters of ZJ-2 oil formation (at the end of model operation).

Table 2: The effect table of liquid extraction for ZJ-1 oil formation.

Well name	Current production			Liquid extraction scheme				Implementation effect		
	Liquid production rate	Oil production rate	Water cut	Liquid extraction rate	Oil extraction rate	Water cut	Draw down	Liquid production rate	Oil production rate	Water cut
	m^3/d		%	m^3/d	m^3/d	%	MPa	m^3/d		%
A6	50	4.3	91.5	500	21.0	95.5	4.6	570	30.2	94.7
A8	911	54.0	94.1	215	6.0	94.7	5.1	1287	70.8	94.5
A2	1757	84.0	95.2	443	10.0	95.7	3.8	2100	98.7	95.3
A7	1273	60.0	95.3	627	16.0	96	4.6	1798	80.9	95.5
A9	399	13.0	96.8	1101	32.0	97	3.8	1659	51.4	96.9
Total	4390	215.3	—	2886	85.0	—	—	7414	332.0	—

the X Oilfield constructed a future development strategy including well production schedule optimization and adjustment wells. For the ZJ-1 main oil group, the existing well pattern control is relatively complete, and the fluid production is optimized in considering well conditions and facility capacity. The focus is on increasing the liquid production rate of wells A6, A8, A2, A7, and A9 in the structural high area (Table 2). For the nonmain oil group, it is proposed to add a new adjustment well as a test well in the area with poor physical properties in the eastern part of the ZJ-2 oil group.

After the implementation of this strategy, the ZJ-1 oil group achieved a daily oil increase of 116.7 m^3/d through an optimized production rate, and the water cut was basically consistent with prediction. When the adjustment well of the ZJ-2 oil group was in production, the initial water cut was 49.0%, and the daily oil production was 190 m^3/d. Then, the water cut reached 91.8% after 7 months of production, and the cumulative oil production was 2.25×10^4 m^3. The oil volume is 11.5×10^4 m^3, and based on the original conventional simulation, the accumulative oil increase of the adjustment wells in this area is only 4.0×10^4 m^3 (Figure 9).

In addition, through core analysis (Figure 10), there is still a pure oil layer about 2 meters thick in the upper part of the ZJ-1 oil formation, and oil in the middle part is moderately displaced. The oil distribution is similar to the core surface of the pure water layer, which indicates that the oil in the middle and lower parts of the reservoir are very well displaced, confirming that strong waterflooding can effectively reduce the residual oil saturation.

4. Conclusions

In this study, based on commercial reservoir simulator, the time-varying simulation of reservoir properties in large field cases was carried out, and a new understanding of remaining oil in ultrahigh water-cut stage was formed. The development strategies were proposed, and the field implementation were tracked. Some conclusions can be obtained as follows:

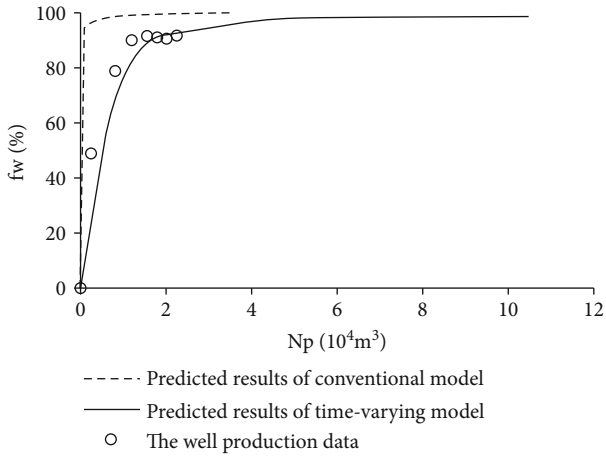

Figure 9: The production performance of the adjustment well in ZJ-2 oil formation.

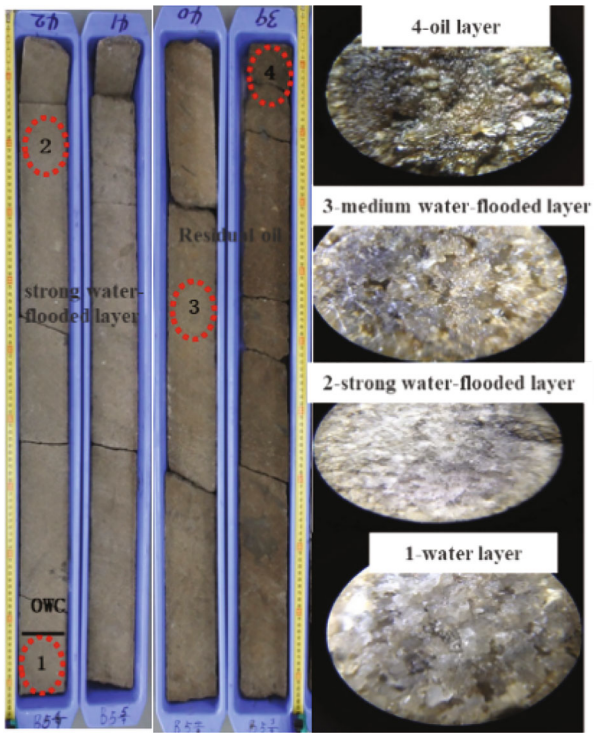

Figure 10: The partial coring section of ZJ-1 oil formation.

(1) The time-varying reservoir properties have a significant impact on the distribution of remaining oil in ultrahigh water-cut reservoir. The time-varying reservoir properties increase the conductivity of strong waterflooding zone, reduce the residual oil saturation, further increase the oil recovery, and correspondingly reduce the recovery of low flooding zone, which makes the remaining oil in the low flooding zone enriched. Compared with the conventional numerical simulation, the remaining oil at the top of the main thick reservoir in the X oilfield is increased by 18.5%. The remaining oil in the low-permeability area at the edge of the nonmain reservoir is increased by 27.3%

(2) Based on the understanding that the time-varying phenomenon of reservoir physical properties affects the distribution of remaining oil in the ultrahigh water-cut stage of the reservoir, a strategy for effectively producing the remaining oil in this stage is proposed. Extracting the remaining oil at the top of the main reservoirs can be achieved by increasing the liquid production rate with existing wells. The new wells can be determined with the assistance of time-varying reservoir simulation and the improvement of understanding of the remaining oil in the low-displacement zone for nonmain reservoirs

Data Availability

All data used to support the findings of this study are available from the corresponding authors on request.

Conflicts of Interest

The authors declare that they have no conflicts of interest.

Acknowledgments

This work is supported by the National Science and Technology Major Project (Grant No. 2016ZX05025-001).

References

[1] K. C. Khilar, R. N. Vaidya, and H. S. Fogler, "Colloidally-induced fines release in porous media," *Journal of Petroleum Science and Engineering*, vol. 4, no. 3, pp. 213–221, 1990.

[2] Q. Feng, J. Zhang, S. Wang et al., "Unified relative permeability model and waterflooding type curves under different levels of water cut," *Journal of Petroleum Science and Engineering*, vol. 154, pp. 204–216, 2017.

[3] Q. Sun Huanquan, F. H. Yantao, and Z. Lunmin, "Formation sensitivity characteristics study of sandstone reservoirs in Shengli oilfield," *Petroleum Exploration and Development*, vol. 27, pp. 72–75, 2000.

[4] L. Yang, "Variation rule of macro parameters and dynamic model of oil reservoirs in continental faulted basin," *Acta Petrolei Sinica*, vol. 26, pp. 65–68, 2005.

[5] J. Bingshan, M. Mingxue, and Q. Xiaoyan, "The mathematical simulation method of migration of fines and clay swell in elastic porous medium," *Research and Development of Hydrodynamics (Part A)*, vol. 18, pp. 9–11, 2003.

[6] W. C. Song, H. Q. Sun, G. Sun, and S. Y. Wu, "Dynamical geological process of development liquid-taking Shengtuo oilfield as an example," *Acta Petrolei Sinica*, vol. 21, pp. 52–55, 2002.

[7] D. Chen, J. Li, W. Zhu, and Z. Xin, "Experimental research on reservoir parameters variation after water flooding for offshore unconsolidated sandstone heavy oil reservoirs," *China Offshore Oil and Gas*, vol. 28, pp. 54–60, 2016.

[8] S. Rui, W. Yao, and L. Jianjun, "Microscopic pore structure characterization and fluid transport visualization of reservoir rock," *Journal of Southwest Petroleum University (Science & Technology Edition)*, vol. 40, pp. 85–105, 2018.

[9] N. Ning, Y. Li, H. Liu, and S. Zhou, "Study on influence of permeability and distribution of pore diameters in rock cores on measurement of mobile fluid saturation," *Journal of Southwest Petroleum University (Science& Technology Edition)*, vol. 40, pp. 91–97, 2018.

[10] W. Zhizhang, C. Yi, and Y. Lei, *The Changing Rule and Mechanism of Reservoir Parameters in the Middle-Later Development Stage*, Petroleum Industry Press, Beijing, 1999.

[11] W. Xin, D. Zong, and W. Hua, "Physical properties of marine sandstone reservoir after long-term waterflooding," *Special Oil and Gas Reservoirs*, vol. 24, pp. 157–161, 2017.

[12] C. Hong, W. Wang, R. Lu, J. Zhong, and C. Ren, "A quantitative method to predict the dynamic variation in permeability of oil reservoirs during waterflooding and oil displacement," *Journal of Southwest Petroleum University (Science& Technology Edition)*, vol. 40, pp. 113–121, 2018.

[13] S. Sun, J. Han, Y. Guo, and W. Zhang, "Laboratory experiment on physical properties of flooding sandstone in Shengtuo oilfield," *Journal of China University of Petroleum.*, vol. 20, pp. 33–35, 1996.

[14] W. Yan, L. Zhengchen, and S. Yang, "Changing rules of well log interpretation permeability in different period in Daqing Placanticline," *Petroleum Geology and Oilfield Development in Daqing*, vol. 21, pp. 60–62, 2002.

[15] O. A. Jalel, "Two-dimensional network model to simulate permeability decrease under hydrodynamic effect of particle release and capture," *Transport in Porous Media*, vol. 37, no. 3, pp. 303–325, 1999.

[16] A. G. Siqueira, E. J. Bonet, and F. S. Shecaira, "A 3D network model of rock permeability impairment due to suspended particles in injection water," in *SPE European Formation Damage Conference*, The Hague, Netherlands, 2003.

[17] G. Changhong, "Understanding capture of non-Brownian particles in porous media with network model," *Asia-Pacific Journal of Chemical Engineering*, vol. 3, no. 3, pp. 298–306, 2008.

[18] L. Huiqing, *Reservoir Numerical Simulation Method*, Petroleum University Press, Shandong, 2001.

[19] H. Q. Jiang, J. W. Gu, M. F. Chen, and M. R. Sun, "Reservoir simulation of remaining oil distribution based on time-variant reservoir model," *Petroleum Exploration and Development*, vol. 32, pp. 91–93, 2005.

[20] C. Z. Cui, Z. L. Geng, Y. Z. Wang, Y. S. Huang, and H. Q. Liu, "Calculation model of dynamic permeability distribution and its application to water drive reservoir at high water cut stage," *Journal of China University of Petroleum*, vol. 36, pp. 118–122, 2012.

[21] Q. Xu, Y. Chen, Y. Hou, and H. Li, "Research on numerical simulation processing mode based on reservoir time varying physical properties and seepage in extra high water cut stage," *Drilling & Production Technology*, vol. 38, pp. 41–43, 2015.

[22] Q. Zhang, R. Jiang, P. Jiang, Z. Yao, Y. Wang, and W. Peng, "Establishment and application of oil reservoir flow-field evaluating system," *Petroleum Geology and Oilfield Development in Daqing*, vol. 33, pp. 86–89, 2014.

[23] R. Jiang, Q. Xin, W. Teng, P. Xu, and Z. Liu, "Numerical simulation of reservoir time-variation based on surface flux," *Special Oil and Gas Reservoirs*, vol. 23, pp. 69–72, 2016.

[24] Y. J. Gai, D. L. Lu, and Y. L. Guo, "Numerical simulation by stages about the reservoir at high water cut period," *Petroleum Geology and Recovery Efficiency*, vol. 7, pp. 54–56, 2000.

[25] G. Boyu, P. Shimi, and H. Shuwang, "Staged numerical simulation of layer 3-member 2-Shahejie formation in district 2 of Shengtuo oilfield," *Petroleum Exploration and Development*, vol. 31, pp. 81–84, 2004.

[26] X. Zhou, F. Al-Otaibi, and S. Kokal, "Relative permeability characteristics and wetting behavior of supercritical CO_2displacing water and remaining oil for carbonate rocks at reservoir conditions," *Energy & Fuels*, vol. 33, no. 6, pp. 5464–5475, 2019.

[27] J. Ruizhong, C. Yueming, D. Yuzhen, and Z. Yan, "Numerical simulation study on the change of physical characteristic parameters of reservoir in the second area of Shengtuo oilfield," *Petroleum Geology and Recovery Efficiency*, vol. 3, pp. 50–56, 1996.

[28] L. Xiantai, "Study on numerical simulation technology based on time varying physical properties in min-high permeability sandstone reservoirs," *Petroleum Geology and Recovery Efficiency*, vol. 18, pp. 58–62, 2011.

[29] Z. Jin, Q. Fang, L. Wang, and L. Zhao, "Numerical simulation method and its application when considering time-dependent effect of reservoir parameters," *Xinjiang Petroleum Geology*, vol. 37, pp. 342–345, 2016.

[30] L. Chen, "Method for calculation the relative permeability curve of an oil reservoir considering the time-varying effect of relevant reservoir parameters," *Journal of Southwest Petroleum University (Science& Technology Edition)*, vol. 41, pp. 137–142, 2019.

[31] Z. Jinqing, *Research on Water Drive Theory and Improvement of Reservoir Engineering Methods*, China petrochemical press, Beijing, 2019.

[32] M. Yue, W. Zhu, H. Han, H. Song, Y. Long, and Y. Lou, "Experimental research on remaining oil distribution and recovery performances after nano-micron polymer particles injection by direct visualization," *Fuel*, vol. 212, pp. 506–514, 2018.

[33] P. Sun, H. Xu, H. Zhu et al., "Investigation of pore-type heterogeneity and its control on microscopic remaining oil distribution in deeply buried marine clastic reservoirs," *Marine and Petroleum Geology*, vol. 123, article 104750, 2021.

[34] W. U. Junda, L. I. Zhiping, and Y. Sun, "Neural network-based prediction of remaining oil distribution and optimization of injection-production parameters," *Petroleum Geology and Recovery Efficiency*, vol. 27, pp. 85–93, 2020.

[35] M. Sun, C. Liu, C. Feng, and G. Zhang, "Main controlling factors and predictive models for the study of the characteristics of remaining oil distribution during the high water-cut stage in Fuyu oilfield, Songliao Basin, China," *Energy Exploration & Exploitation*, vol. 36, no. 1, pp. 97–113, 2018.

[36] Y. Yang, S. Cai, J. Yao et al., "Pore-scale simulation of remaining oil distribution in 3D porous media affected by wettability and capillarity based on volume of fluid method," *International Journal of Multiphase Flow*, vol. 143, article 103746, 2021.

[37] R. Li, K. D. Splinter, and S. Felder, "Aligning free surface properties in time-varying hydraulic jumps," *Experimental Thermal and Fluid Science*, vol. 126, article 110392, 2021.

[38] M. Hashan, L. N. Jahan, S. Imtiaz, and M. E. Hossain, "Modelling of fluid flow through porous media using memory approach: a review," *Mathematics and Computers in Simulation*, vol. 177, pp. 643–673, 2020.

[39] I. Igwe, J. Gholinezhad, and M. Sayed, "Technical implications of neglecting compositional grading effects in petroleum reservoir simulation models," *Energy & Fuels*, vol. 34, no. 2, pp. 1467–1481, 2020.

[40] H. F. Xia, L. I. Wen-Zhuo, Y. Liu, H. Y. Zhang, and X. U. Tian-Han, "Quantitative analysis of remaining oil after weak base alkaline-surfactant-polymer flooding," *Science Technology and Engineering*, vol. 19, pp. 127–131, 2019.

[41] S. Zhai, G. Sun, H. Chang, Q. Wu, and Y. Lei, "Study on remaining oil distribution of shallow water delta reservoir in horizontal well development: an example from Bohai oilfield," *Journal of Liaoning Shihua University*, vol. 39, pp. 53–58, 2019.

[42] Z. Zhu, "Remaining oil distribution patterns of metamorphic buried-hill fractured reservoir based on digital core technology," *Special Oil & Gas Reservoirs*, vol. 26, p. 157, 2019.

[43] S. Gao, S. Chen, H. Pu et al., "Fine characterization of large composite channel sandbody architecture and its control on remaining oil distribution: a case study of alkaline-surfactant-polymer (ASP) flooding test area in Xingshugang oilfield, China," *Journal of Petroleum Science & Engineering*, vol. 175, pp. 363–374, 2019.

[44] L. U. Xiangwei, D. U. Shuheng, K. Zheng, H. Zhang, T. Sun, and H. Wang, "Fracture development characteristics in tight sandstone oil reservoir and its inspiration on remaining oil recovery: a case study on the Chang-7_2~2 layer of Yanchang Formation in Xin'anbian area, Ordos Basin," *Acta Scientiarum Naturalium Universitatis Pekinensis*, vol. 54, pp. 42–48, 2018.